NASA/TM—2004-212332

Infrared Heater Used in Qualification Testing of International Space Station Radiators

Robert A. Ziemke
Glenn Research Center, Cleveland, Ohio

May 2004

The NASA STI Program Office . . . in Profile

Since its founding, NASA has been dedicated to the advancement of aeronautics and space science. The NASA Scientific and Technical Information (STI) Program Office plays a key part in helping NASA maintain this important role.

The NASA STI Program Office is operated by Langley Research Center, the Lead Center for NASA's scientific and technical information. The NASA STI Program Office provides access to the NASA STI Database, the largest collection of aeronautical and space science STI in the world. The Program Office is also NASA's institutional mechanism for disseminating the results of its research and development activities. These results are published by NASA in the NASA STI Report Series, which includes the following report types:

- TECHNICAL PUBLICATION. Reports of completed research or a major significant phase of research that present the results of NASA programs and include extensive data or theoretical analysis. Includes compilations of significant scientific and technical data and information deemed to be of continuing reference value. NASA's counterpart of peer-reviewed formal professional papers but has less stringent limitations on manuscript length and extent of graphic presentations.

- TECHNICAL MEMORANDUM. Scientific and technical findings that are preliminary or of specialized interest, e.g., quick release reports, working papers, and bibliographies that contain minimal annotation. Does not contain extensive analysis.

- CONTRACTOR REPORT. Scientific and technical findings by NASA-sponsored contractors and grantees.

- CONFERENCE PUBLICATION. Collected papers from scientific and technical conferences, symposia, seminars, or other meetings sponsored or cosponsored by NASA.

- SPECIAL PUBLICATION. Scientific, technical, or historical information from NASA programs, projects, and missions, often concerned with subjects having substantial public interest.

- TECHNICAL TRANSLATION. English-language translations of foreign scientific and technical material pertinent to NASA's mission.

Specialized services that complement the STI Program Office's diverse offerings include creating custom thesauri, building customized databases, organizing and publishing research results . . . even providing videos.

For more information about the NASA STI Program Office, see the following:

- Access the NASA STI Program Home Page at ***http://www.sti.nasa.gov***

- E-mail your question via the Internet to help@sti.nasa.gov

- Fax your question to the NASA Access Help Desk at 301–621–0134

- Telephone the NASA Access Help Desk at 301–621–0390

- Write to:
  NASA Access Help Desk
  NASA Center for AeroSpace Information
  7121 Standard Drive
  Hanover, MD 21076

NASA/TM—2004-212332

Infrared Heater Used in Qualification Testing of International Space Station Radiators

Robert A. Ziemke
Glenn Research Center, Cleveland, Ohio

National Aeronautics and
Space Administration

Glenn Research Center

May 2004

Acknowledgments

The author wishes to thank Nabil Kattouah for his design of the heater array support structure, Todd Schroeder and his crew for the buildup and alignment of the infrared lamp assemblies, and Wayne Lenhart for suggesting the use of flexible jumpers to eliminate the arcing at the lamp module clamps. These dedicated people and others contributed greatly to the success of the infrared heater system.

Available from

NASA Center for Aerospace Information
7121 Standard Drive
Hanover, MD 21076

National Technical Information Service
5285 Port Royal Road
Springfield, VA 22100

Available electronically at http://gltrs.grc.nasa.gov

Infrared Heater Used in Qualification Testing of International Space Station Radiators

Robert A. Ziemke
National Aeronautics and Space Administration
Glenn Research Center
Cleveland, Ohio 44135

Introduction

Two heat rejection radiator systems for the International Space Station (ISS) have undergone thermal vacuum qualification testing at the NASA Glenn Research Center (GRC), Plum Brook Station, Sandusky, Ohio. The testing was performed in the Space Power Facility (SPF), the largest thermal vacuum chamber in the world.

The heat rejection system (HRS) radiator was tested first; it removes heat from the ISS crew living quarters. The second system tested was the photovoltaic radiator (PVR), which rejects heat from the ISS photovoltaic arrays and the electrical power-conditioning equipment. The testing included thermal cycling, hot- and cold-soaked deployments, thermal gradient deployments, verification of the onboard heater controls, and for the PVR, thermal performance tests with ammonia flow. Both radiator systems are orbital replacement units (ORU) for ease of replacement on the ISS. The terms ORU and radiator will be used synonymously throughout the remainder of this report.

One key to the success of these tests was the performance of the infrared heater system. It was used in conjunction with a gaseous-nitrogen-cooled cryoshroud in the SPF vacuum chamber to achieve the required thermal vacuum conditions for the qualification tests. The heater, which was designed specifically for these tests, was highly successful and easily met the test requirements. This report discusses the heating requirements, the heater design features, the design approach, and the mathematical basis of the design.

The design mathematics have been improved since the heater was built. This report presents the improved mathematical treatment and then briefly discusses the original treatment.

Deployment Test Setup

The stowed ORU was mounted at one end of the deployment track (ref. 1). The track provided the mechanical support needed to horizontally deploy and retract the radiator panels in the one-gravity environment. The heater consisted of planar arrays of infrared (IR) tungsten quartz lamps surrounding the stowed ORU (fig. 1). The ORU, deployment fixture, and heater were all enclosed by the cryoshroud inside the SPF vacuum chamber (ref. 2).

The front of the heater was designed to swing open to provide an unobstructed path for radiator deployment. Remotely operated lamp array doors were provided for this purpose. Figure 2 shows the heater with its doors open just prior to deployment.

Thermal Requirements

The infrared heater was required to perform the following functions (refs. 3 and 4):

1. Uniformly heat the stowed ORU at a sufficient rate (approximately 1 deg F/min) to various steady-state temperatures over a range of –125 to +140 °F with the cryoshroud temperature as low as –160 °F.

2. Trim and maintain the ORU temperature during the 12-hr hot- and cold-soak periods.

3. Generate the required thermal gradients (160 deg F max.) across opposite faces of the stowed ORU by applying heat from the lamp array to one side of the ORU and allowing the opposite side to lose heat by radiation to the cryoshroud.

4. Provide backup heat if needed to the ORU base during testing of the onboard heater control assembly.

For each ORU surface, the radiator manufacturer, Lockheed Martin Vought Systems (LMVS), calculated the incident heat flux density needed to produce the desired heating rate (1 deg F/min), taking into account the surface emissivity under incandescent tungsten illumination. Table I shows the heat flux densities for all surfaces of the stowed ORU as the flux-required values (ref. 3). A design margin of approximately 50 percent was added to the required values. The margin allowed for

1. Uncertainty in the ORU surface emissivities under incandescent tungsten illumination

2. Possible long-term degradation of the infrared lamps and/or reflectors

The flux-with-margin values shown in table I were given to NASA as test facility requirements and were used to size and design the lamp arrays. The flux-with-margin values for the base and panel surfaces were later increased by LMVS to 132 and 281 W/ft^2, respectively, and the design of the corresponding heater arrays was modified accordingly. No quantitative requirements were given for heat flux uniformity. Temperature uniformity across each ORU surface was the more critical issue.

The ORU surfaces are composed of metallic materials of relatively high thermal conductivity, which tend to minimize surface temperature gradients caused by nonuniform flux density. Also, temperature gradients are minimal during the critical predeployment soak periods because the flux density is low when the heater system is holding the ORU surface temperature constant. For these reasons flux uniformity was not considered to be a major driver in the heater design. However, it was decided to make a reasonable attempt by using limited analysis tools to design the arrays to theoretically produce good flux uniformity.

Because the heat flux density requirements included a large margin and flux uniformity was not critical, it was decided at the outset to evaluate heater performance on the basis of mathematical analysis only, and not to expend the great amount of resources needed to optically scan the arrays. Early in the development a high confidence in the mathematical analysis was gained when the IR lamp vendor independently sized an array and the results agreed with the analysis prediction.

Heater Description

The heater arrays collectively consisted of 203 quartz line-source tungsten filament lamps. These lamps were a combination of 5-in., 120-V, 500-W and 10-in., 240-V, 1000-W Research Inc. Model 5236

space thermal simulation modules (ref. 5). These lamp modules (fig. 3) featured gold-plated reflectors. Figure 7(a), an excerpt from the manufacturers literature, shows the radiation spectrum of the Model 5236. The lamp modules were arranged in six independent planar arrays, one array for each face of the stowed ORU. Independent closed-loop temperature control based on ORU surface temperature (type T thermocouple) was provided for each ORU face (zone) and its corresponding array. The lamp modules were rigidly mounted on aluminum channels and were spaced along the channel length with the filaments oriented perpendicular to the channel (fig. 4). These assemblies were individually bench assembled, prewired, and later installed in modular fashion to form columns on the heater support structure.

The heater support structure was fabricated of heavy-gauge aluminum channels and beams. The larger-surface-area components were covered with high-emissivity plastic tape to enhance the structure's cooldown rate in preparation for the cold-soak periods. The aluminum support structure was sized primarily to accommodate the HRS radiator (approximate stowed envelope dimensions: 141 in. high by 104 in. wide by 32 in. deep). The structure was made mechanically adjustable so that the smaller photovoltaic radiator could also be accommodated.

To simplify the wiring on the high-flux zones (ORU panel surface and base), aluminum bus rods (0.5-in. diameter) were used to distribute the electrical power to the lamps. The lamps were wired in a three-phase wye configuration. A provision was made in the design to allow for differences in thermal expansion of the bus rods and the aluminum structure. This allowance was accomplished by reducing the clamping force on the lamp module bus bar clamps so that they were free to slide on the bus rods. Flexible jumper wires were connected from the clamps to the bus rods to provide a low-resistance electrical path as shown in figure 4. The insulated bus rod supports (fig. 5) provided vertical restraint for the bus rods to prevent mechanical creeping of the rods due to the sliding action of the clamps during thermal cycling.

The lamp filament voltage was reduced on the low-flux zones (ORU top, bottom, and sides) to permit using a sufficient number of lamps to achieve good flux uniformity without greatly exceeding the flux density requirement. This voltage reduction was accomplished by wiring the lamps in a three-phase delta configuration with several lamps in series per leg. This arrangement allowed the silicon-controlled rectifier (SCR) power controllers assigned to the low-flux zones to operate at a voltage comparable to that of the high-flux-zone controllers, while still providing a reduced voltage to the individual lamps.

Electrical Power Supply

Six existing 480-V, 400-kW, remote-controlled, three-phase, water-cooled SCR power controllers of the phase-angle control type were used. The fusing and current sensing were scaled down to match the actual heater electrical loads. Thermac* temperature controllers provided manual and automatic proportional-integral-differential (PID) closed-loop temperature control for each zone. Remote meter indication of power level was also provided. Current limiting was used to reduce filament in-rush current. Voltage limiting was used to control the rate of ORU temperature rise, to reduce overshoot, and to lessen the stress on the infrared lamp filaments.

Diesel generator backup power was provided for the lamps that heated the ORU base. This backup was intended to protect the onboard electronics from extreme cold in the event of a power failure.

*Thermac is a registered trademark of Research Inc., Eden Prairie, MN.

Checkout

The SCR power controllers were initially checked out and adjusted in the manual mode with a dummy load. After the ORU and infrared lamp arrays were installed in the test chamber, an in-air test was performed. The lamp arrays were manually energized one at a time. The ORU surface temperatures were continuously monitored, and caution was exercised to ensure that the temperatures did not exceed 120 °F. After a brief cooldown period the infrared heater system was then operated in the automatic closed-loop temperature control mode with the set points at various temperatures up to 110 °F. The PID adjustments were optimized for best step response and minimum overshoot. The manual and automatic closed-loop tests were repeated with the test chamber at vacuum. Minor PID readjustments were made to compensate for the lack of convective heat loss.

Problems Encountered

The original heater array design used sliding electrical contact between the lamp module clamps and the aluminum bus rods to allow for differences in thermal expansion of the components. During early testing in vacuum at extremely low temperatures the integrity of the sliding contact for some of the lamps deteriorated sufficiently to cause arcing at the contact point. It is believed that the arcing generated a highly ionized metal plasma that quickly engulfed the entire heater array, shorting out all six zones. This short circuit caused the protective fuses in all six power controllers to blow. The problem was solved by connecting flexible jumper wires from the lamp module clamps to the bus rods. This arrangement still allowed the clamps to slide but eliminated the arcing by providing a low-resistance current bypass. Later, a similar plasma-induced breakdown occurred when a nearby video camera light fixture developed an electrical short and the ensuing arc emitted a metal plasma toward the energized heater array. Again, the array shorted out after it became engulfed in the plasma.

These events underscore the fact that any high-voltage electrical device with exposed conductors in a high vacuum is vulnerable to breakdown due to external incidental plasma sources. Such sources should be eliminated by careful design, thorough inspection, and checkout.

Heater Performance

The ORU surface temperature response was much quicker than expected, most likely because of the 50-percent design margin. Stable closed-loop temperature control was easily achieved. The required heating rate of 1 deg F/min (for thermal cycling) was easily met with the cryoshroud temperature as low as –160 °F. The pretest heat-soak conditioning was achieved in less than the required 12 hr. The required thermal gradient test conditions were satisfactorily achieved.

Lamp Array Design Approach

It became apparent early on that an iterative approach would be appropriate for the task of designing the arrays. The key component needed was a computer algorithm that would enable the designer to theoretically see how lamp array geometry adjustments affect the incident flux produced. Equipped with this tool the designer would then incrementally adjust the array geometry on the basis of the calculated result

to ultimately achieve the desired flux density and uniformity at the receiving plane. The radiation mathematics was developed and incorporated into finite element analysis computer programs designed for each array. These programs provided the needed feedback to the designer.

The lamp filaments were divided into 1-in. segments. The incident flux density at the receiving plane (one face of the stowed ORU) was calculated at equally spaced points along selected vertical and horizontal scan lines. The calculated flux density at each point was a summation of flux contributions from each segment of all lamp filaments within the zone. The incident flux along these scan lines was evaluated on the basis of the average flux density and uniformity. The incident flux uniformity was then optimized by manually adjusting both the lamp-to-lamp spacing and the relative distance of the lamps to the receiving plane until, after repeated trials, the desired uniformity and average flux density were simultaneously obtained, based on the finite element analysis results.

As the array design proceeded, it became apparent that the achievable flux uniformity was limited because of the following factors:

1. The number of lamps per array was limited.

2. For practical reasons, it was necessary to arrange the lamps in discrete rows and columns, thus limiting the degrees of freedom available in positioning the lamps within the arrays.

3. The finite (nonzero) length of the lamp filaments tended to degrade flux uniformity in the direction parallel to the filament axis.

The effects of these factors will be seen in the design example presented later in this report.

Finite Element Analysis

Figure 6 shows the receiving plane at a distance Z from and parallel to the heater array plane. Each filament segment (source element) was treated as a point source because the minimum radiation path length to the receiving plane was large (more than 10 times the length of the segment). The normal radiant flux density produced by each source element is given by

$$R = JP(L/F) \qquad \text{W/steradian} \tag{1}$$

where J is the lamp radiant flux density modulus in watts per steradian per kilowatt of input, P is the lamp power input in kilowatts, L is the source element length in inches, and F is the total filament length in inches. The value of J given in the manufacturer's literature, figure 7(b), is approximately 160 W/steradian-kW input (ref. 5). With a 10-in. lamp operating at full power (1 kW) and an element length of 1 in., the value of R for each element becomes 16 W/steradian.

In calculating the incident flux at the receiving plane, the following assumptions were made:

1. The received radiant flux density is proportional to the inverse square of the distance from the receiving point to the center of the source element.

2. The received radiant flux density is proportional to the cosine of the angle of incidence.

3. The received radiant flux density is proportional to the sine of the angle from the flux path to the element axis (source element tilt). See figure 7(b).

4. The received radiant flux density is independent of the receiving point orientation about the element axis (radial orientation). See figure 7(b).

The effect of the shadow cast by the lamp reflector at large angles of incidence was neglected because the contribution of incident flux at large angles is negligibly small at the receiving plane.

On the basis of these assumptions the incident flux density E in watts per square inch at any point on the receiving plane is given by the following summation, which includes the contributions of all lamp filament source elements from all the lamps within the zone:

$$E = \sum \frac{DGR}{S^2} \tag{2}$$

where the distance from the source element center to the receiving point in inches is

$$S = \left[\left(A - X \right)^2 + \left(B - Y \right)^2 + Z^2 \right]^{0.5} \tag{3}$$

the attenuation factor due to the angle of incidence at the receiving point is

$$D = \frac{Z}{S} \tag{4}$$

the attenuation factor due to source element tilt is

$$G = \frac{V}{S} \tag{5}$$

the distance from the source element axis to the receiving point in inches is

$$V = \left[\left(B - Y \right)^2 + Z^2 \right]^{0.5} \tag{6}$$

and X,Y are the coordinates of the receiving point in inches, A,B,Z are the coordinates of the source element center in inches, R is the normal radiant flux density per source element in watts per steradian, and Z is the distance between the receiving plane and the heater array plane in inches. Figure 8 shows the geometrical relationship of the source element to the receiving point as described by equations (3) to (6).

Lamp Array Design Example

The following steps describe the procedure used to design the array for zone 2 (panel surface). The arrays for the other five ORU faces were designed by using a similar procedure. Zone 2 was unique in that it was divided into two subarrays, each forming one-half of the double-door arrangement needed to provide clearance for deployment.

1. The nominal distance from the lamp filaments to the ORU surface was established. A distance of 18 in. was selected as a good compromise between acceptable envelope size and the ability to maintain an acceptable lamp-to-ORU distance tolerance.

2. Of the three lamp sizes available (5-, 10-, and 16-in. heated lengths), the 10-in. size was selected as the best compromise considering cost, ruggedness, radiation flux density, and the ratio of filament length to array width.

3. A hypothetical lamp array, with the lamps operating at full power and uniformly spaced vertically and horizontally, was sized to the approximate dimensions of the ORU panel surface. Then the number and spacing of the lamps were varied until the finite element analysis, performed along a scan line running vertically down the central portion of the panel surface, indicated the average flux density to be approximately equal to the required flux-with-margin value from table I. The vertical scan line, which ran the full height of the panel, was centered under one of the innermost columns of lamp filaments. Note that because of symmetry, only one quadrant of the panel surface need be considered in the analysis.

4. The total number of lamps was then adjusted to be a multiple of six so that the array could be configured electrically as two symmetrical three-phase wye loads, with half of the lamps assigned to each door.

5. Steps 3 and 4 were repeated as necessary to achieve the approximate required average flux-with-margin density from the multiple-of-six array. Figure 9 (curve A) shows the resulting flux distribution. Note that even though the lamps were uniformly spaced, the flux density fell off rather rapidly each side of center.

6. To compensate for the falloff, a lamp-spacing gradient was introduced vertically within the columns whereby the lamps near the column center were spaced farther apart and the lamps near the column ends were spaced closer together. Figure 9 (curve B) shows the result after iterative optimization.

7. To compensate for the remaining flux density sag near the edges, the edge lamps were moved 3 in. closer to the ORU panel surface. Further iterative optimization produced the result shown in figure 9 (curve C).

8. A similar spacing gradient was then introduced in the horizontal direction by adjusting the column spacing. As before, the lamps of the edge columns were moved 3 in. closer to the ORU panel surface to minimize flux density sag near the edges. The flux density was analyzed along a horizontal scan line centered under the innermost row of lamp filaments, and the horizontal spacing of the columns was optimized. The result is shown in figure 10. Note that the flux uniformity in the horizontal direction (fig. 10) was not as good as that obtained in the vertical direction (fig. 9, curve C). The increased residual ripple in the flux density was a result of the relatively large horizontal distance between the columns. Also, the length of the filaments lessened the effectiveness of the column spacing gradient, as evidenced by a small residual flux density falloff each side of center.

9. It was observed that horizontal spacing adjustments had a small effect on the vertical flux distribution and vice-versa. Therefore, the horizontal and vertical analyses and optimizations were repeated as necessary to obtain a satisfactory flux distribution in both directions simultaneously.

In addition to the above analyses covering the central portion of the array, the finite element analysis was performed along the edges, along scan lines centered under the lamp filaments, and midway between filaments in an attempt to evaluate the flux distribution over the entire ORU panel surface. Figures 11 and 12 show the predicted heat flux distribution along the edge, intermediate, and center scan lines.

No attempt was made to further reduce flux falloff at the corners. Figure 13 shows the resulting lamp layout for zone 2 superimposed on the ORU panel. Note that all peripheral lamps were located 3 in. closer to the panel surface.

Figure 14 shows how the predicted flux density at 3657 points sampled on the ORU panel surface deviated from the predicted mean density of the flux incident on the panel. The points were located on a 2-in.-by-2-in. grid covering the entire panel surface. In figure 14 the calculated deviations were sorted into six bands, each representing a 5-percent incremental deviation from the mean flux density. It can be seen that a relatively small number of points indicated deviations greater than 10 percent.

Original Heater Design

The original design used a mathematical treatment identical to the one just described except that the source element tilt attenuation factor G was not calculated according to equations (3), (5), and (6) but was calculated as follows:

$$G = \frac{Z}{\left[\left(A - X\right)^2 + Z^2\right]^{0.5}} \tag{7}$$

This less accurate two-dimensional calculation of G does not take into account the Y component of the tilt. The three-dimensional expression for G (eqs. (3), (5), and (6)) was not developed until after the lamp arrays had been designed, built, and installed in the SPF test chamber and the first series of HRS and PVR deployment tests had been completed. The use of equation (7) in the original design resulted in a small (less than 4 percent) degradation in predicted flux uniformity, which did not affect the heater's ability to meet the test requirements. Figures 15 and 16 show the potential improvement in flux uniformity offered by the new design compared with the original design. Equations (1) to (6) were used in the performance analysis of both designs to generate these plots.

Because the heater as originally designed met the test requirements, it was decided to continue to use the heater without modification for the balance of the test program and not upgrade to the new design. The heater as originally designed performed exceedingly well and pleased the test customer (LMVS) throughout the entire radiator development and qualification test program.

References

1. Voss, F.E.: Thermal Vacuum Qualification Testing for the International Space Station Heat Rejection System Radiators. SAE Paper 98ES–34, July 1998.
2. Beach, D.E.; et al: Thermal Vacuum Testing of the Heat Rejection System Radiator for the International Space Station. Paper presented at the Twenty-first Space Simulation Conference: The Future of Space Simulation Testing in the 21st Century, 2000, pp. 49–57.
3. Test Requirements Document for HRS Tests at NASA Lewis Plum Brook Space Power Facility, LV Report No. 3–47300H/6R–005, April 9, 1996.
4. Test Procedure for Space Station HRS Radiator Thermal Vacuum Test at NASA Lewis Plum Brook Space Power Facility, LV Report No. 3–47300H/6R–018, Rev. C., Sept. 22, 1997.
5. Model 5236 Space Thermal Simulation Module, Product Data Sheet 5516–D–01–C, Research Inc., 1995.

TABLE I.—HEAT FLUX DENSITY REQUIREMENTS[a]

Surface	Dimensions, in.	Flux required, W/ft^2	Flux with margin, W/ft^2
(a) For hot deployment at 140 °F and ambient cryoshroud from stowed position			
Top	104 by 32.2	49.3	75
Bottom	104 by 32.2	49.3	75
Sides (2)	141 by 32.2	49.3	75
Panel surface	134.8 by 104	174	260
Base	141 by 104	49.3	75
(b) For differential temperature deployment where bottom surface is 200 deg F higher than opposite side[b]			
Bottom	104 by 32.2	77.8	117

[a]±5 deg F requested variation in environment temperature across a surface.
[b]Bottom surface includes scissors beam, hinges, and portion of base. It does not include panel manifold extrusions. ORU stabilized at –100 °F, bottom of ORU heated to 100 °F, and cryoshroud at –150 °F.

Figure 1.—Stowed heat rejection system orbital replacement unit inside infrared heater.

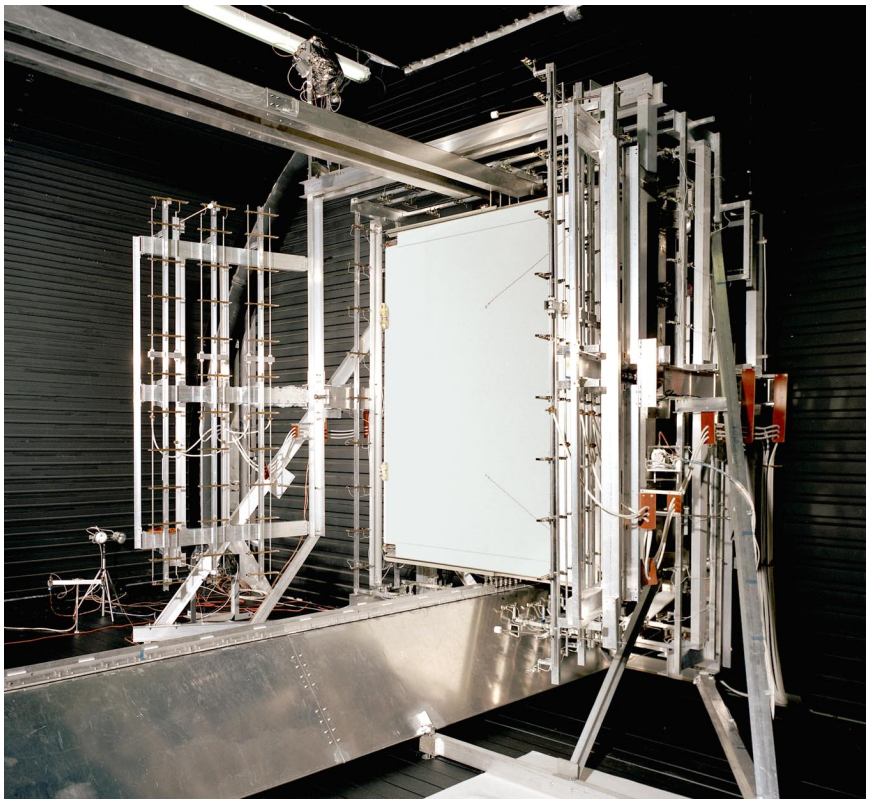

Figure 2.—Infrared heater with doors open.

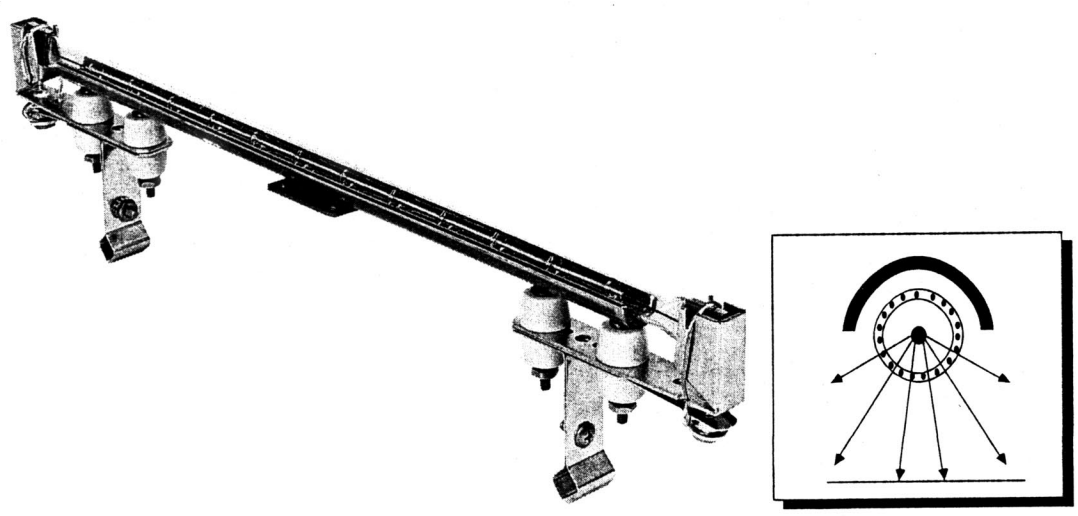

Figure 3.—Model 5236 space thermal simulation module (ref. 5).

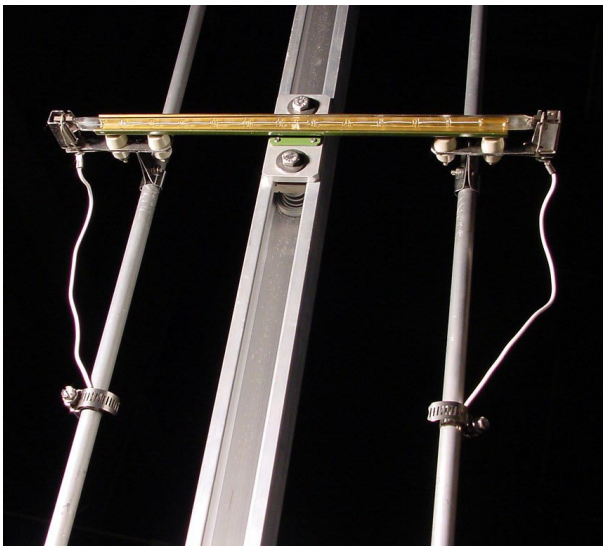

Figure 4.—Infrared heat lamp mounting and electrical connections.

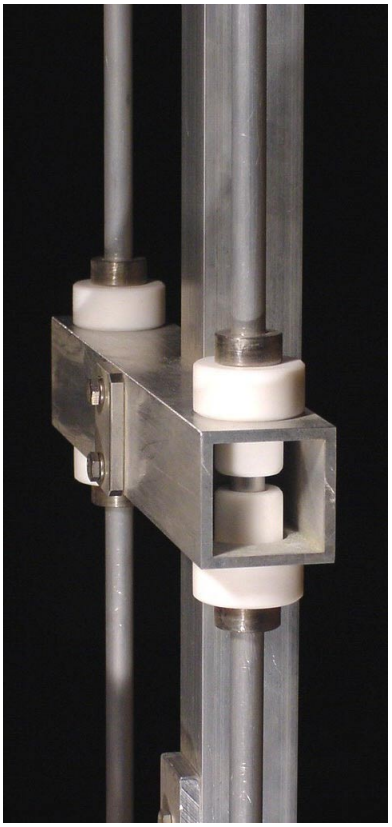

Figure 5.—Insulated bus rod supports.

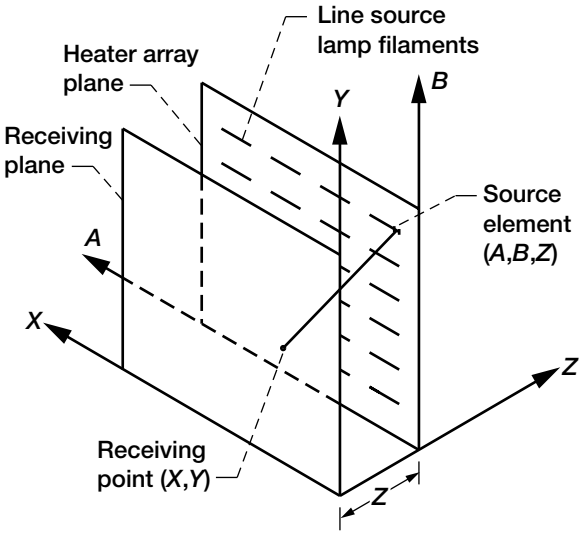

Figure 6.—Typical zone configuration.

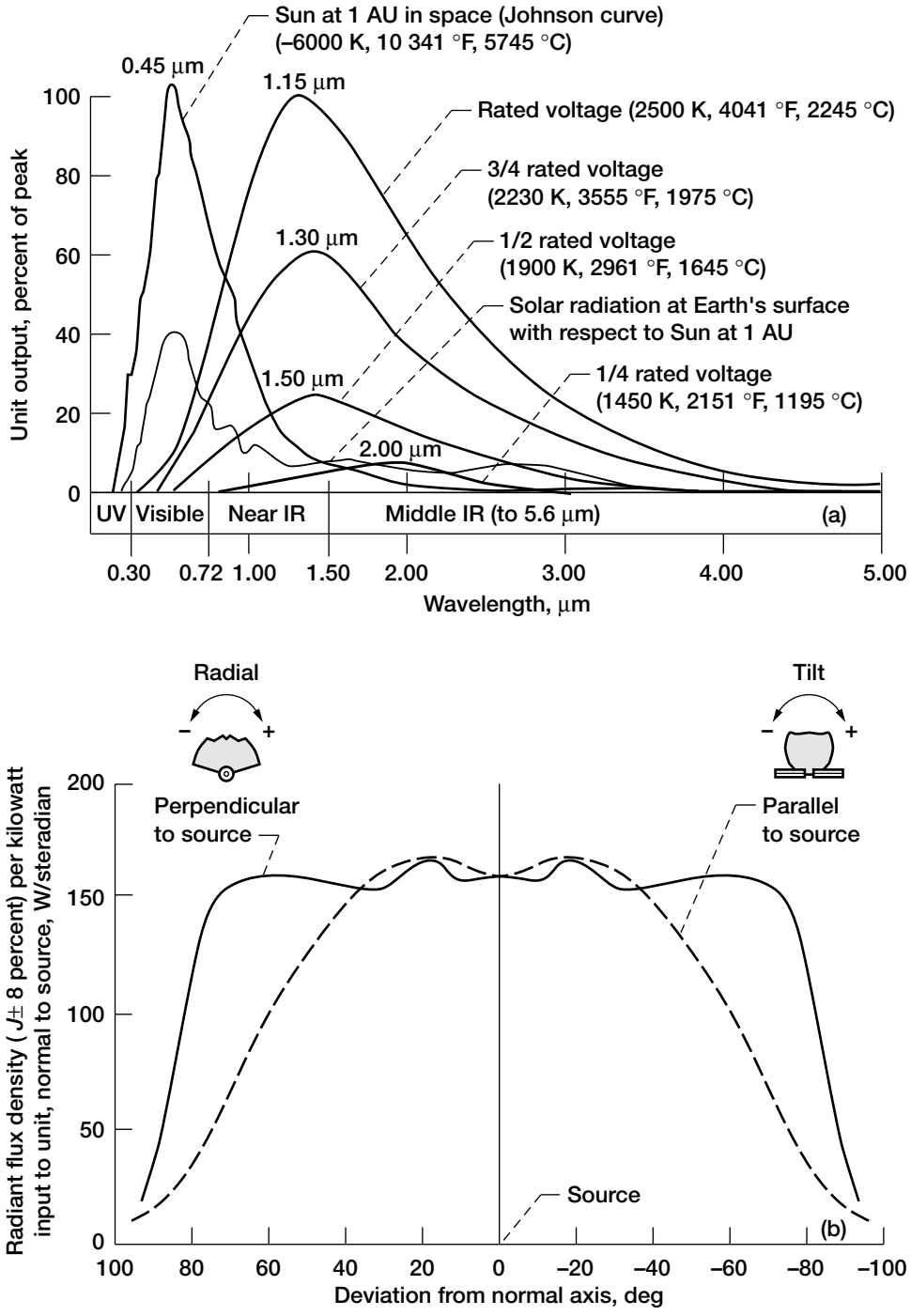

Figure 7.—Radiation characteristics of Model 5236. (a) Spectral output. (b) Directional response.

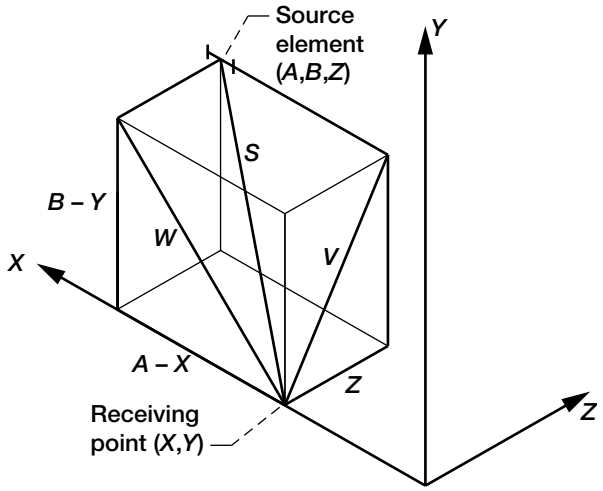

Figure 8.—Element geometry.

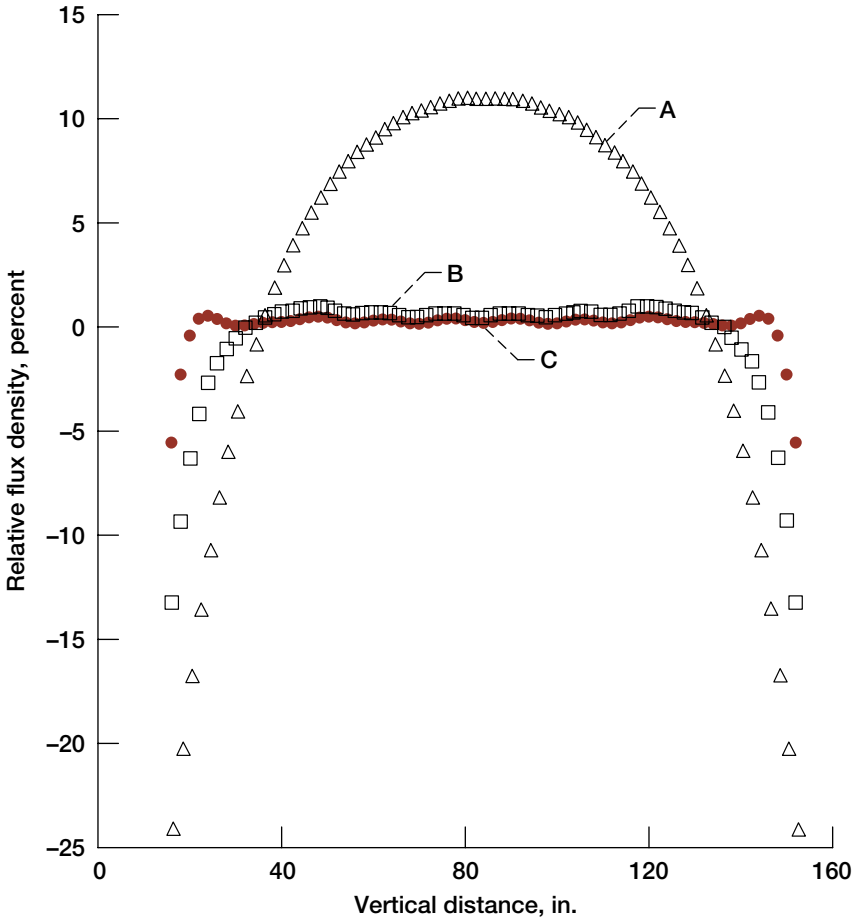

Figure 9.—Predicted heat flux distribution along central vertical scan line (X = 49.8 in.).

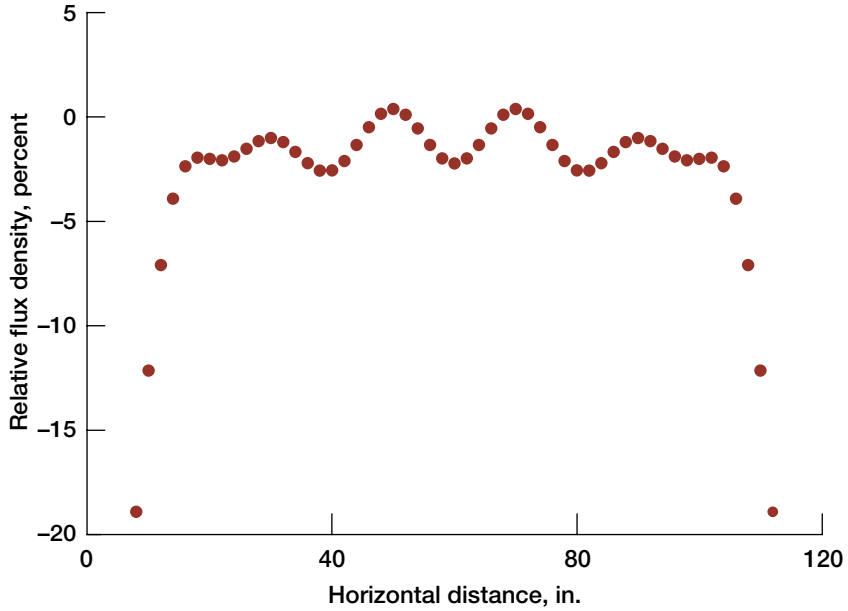

Figure 10.—Predicted heat flux distribution along central horizontal scan line (Y = 76.9 in.).

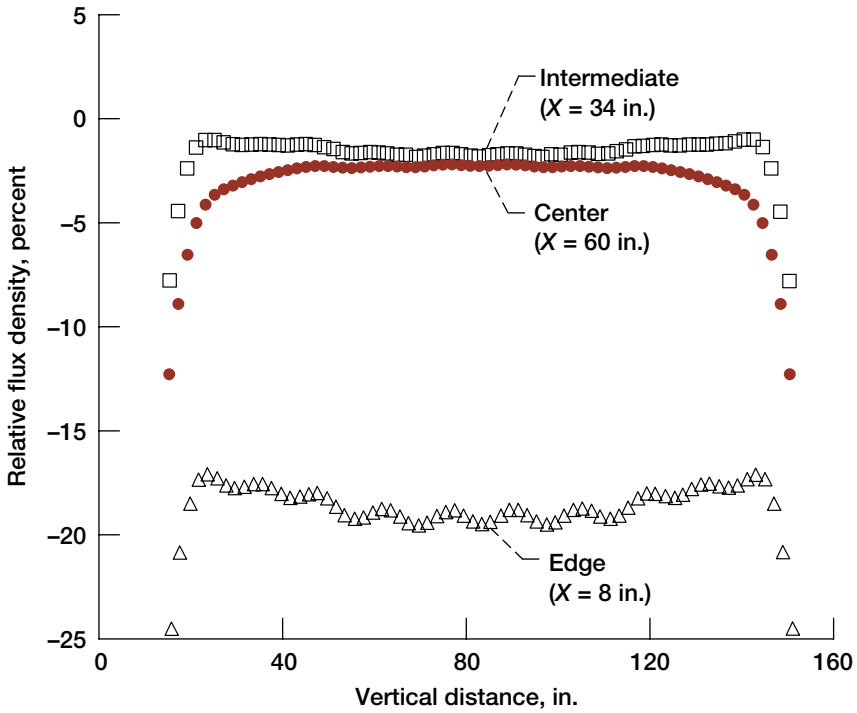

Figure 11.—Predicted heat flux distribution along edge, intermediate, and center vertical scan lines

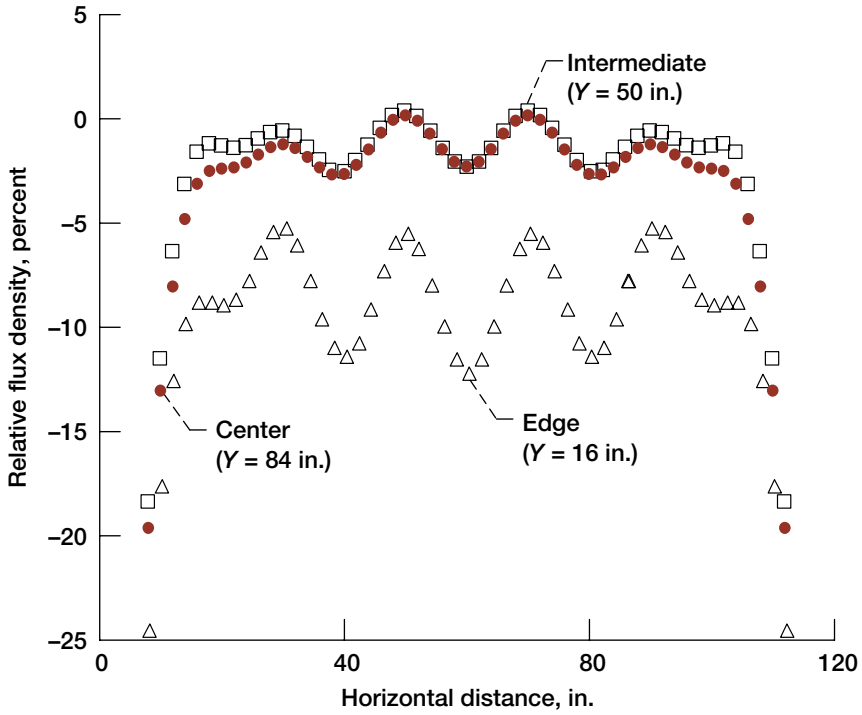

Figure 12.—Predicted heat flux distribution along edge, intermediate, and center horizontal scan lines

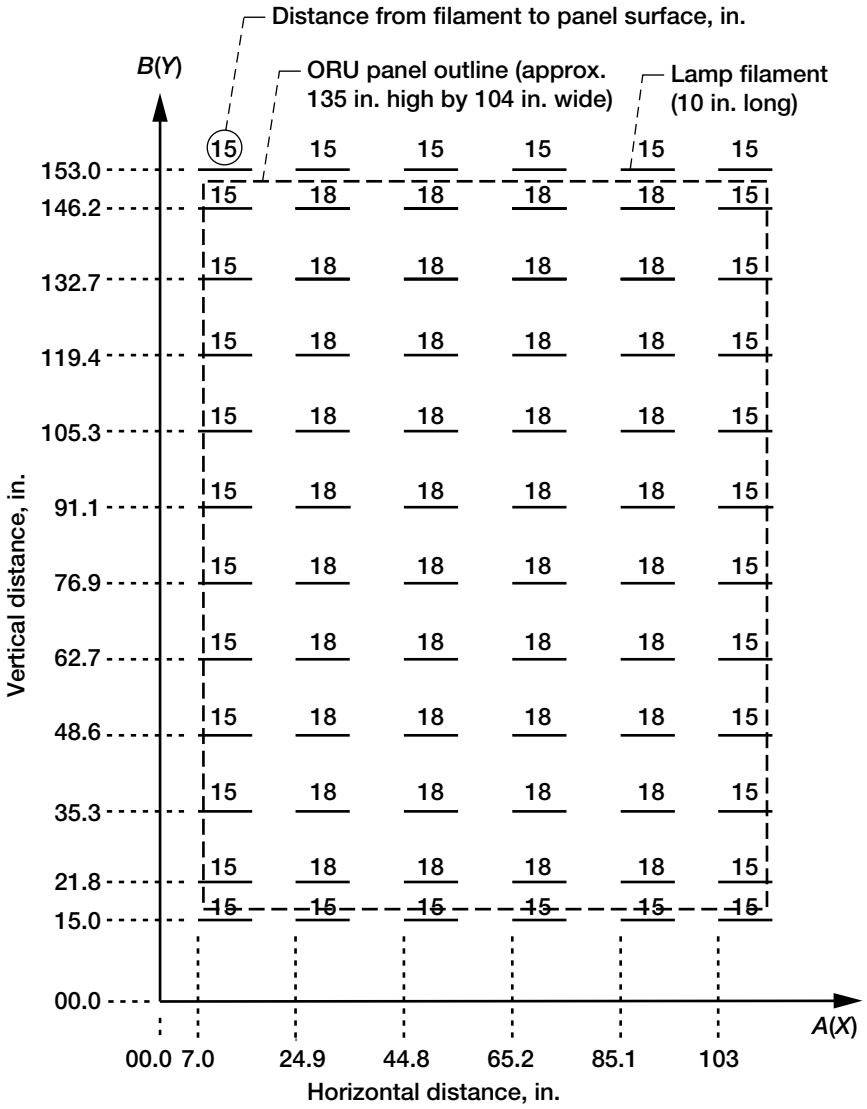

Figure 13.—Lamp layout for zone 2.

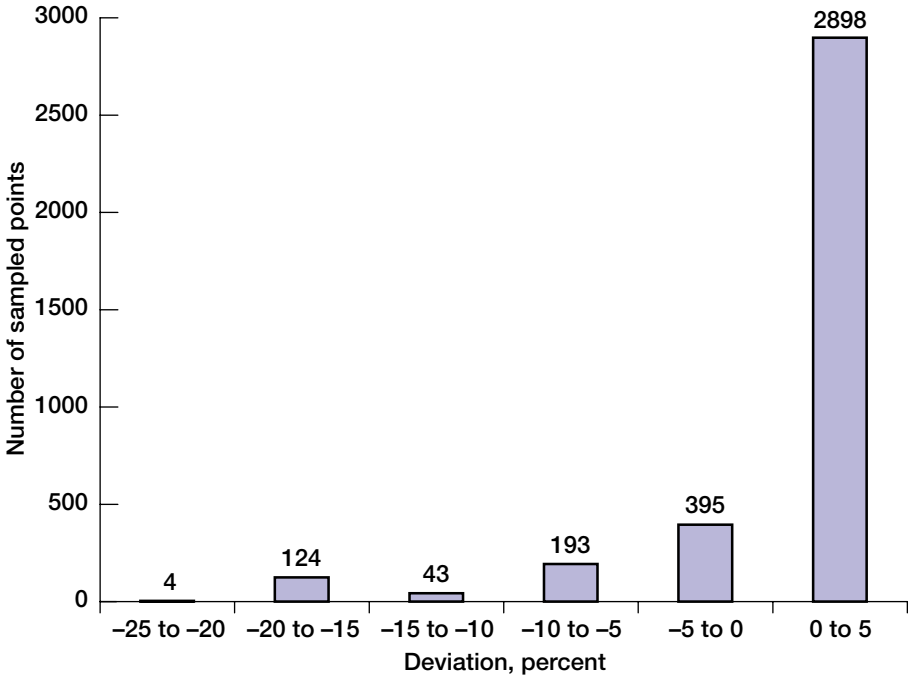

Figure 14.—Predicted deviation from average heat flux density.

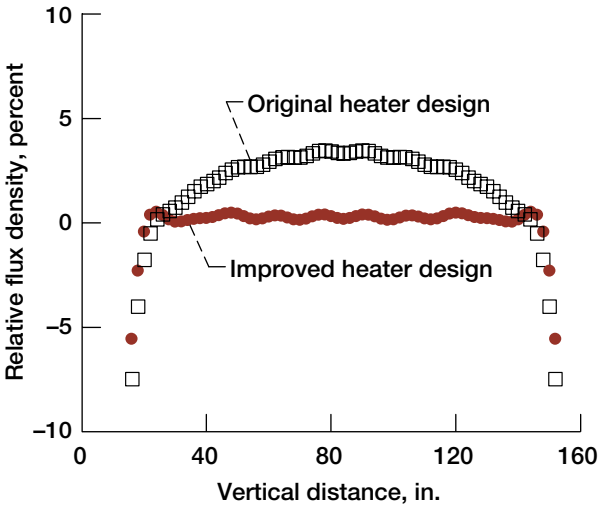

Figure 15.—Predicted heat flux distribution along central vertical scan line (X = 49.8 in.).

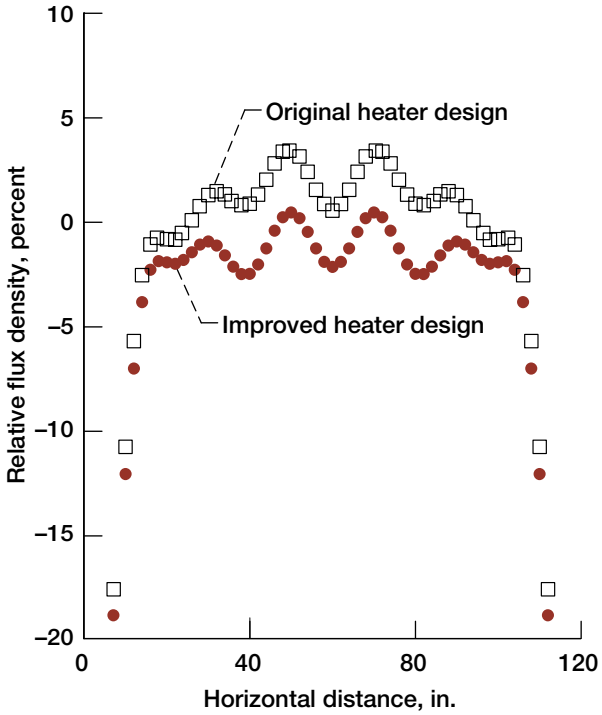

Figure 16.—Predicted heat flux distribution along central horizontal scan line (Y = 77.0 in.).

REPORT DOCUMENTATION PAGE

Form Approved
OMB No. 0704-0188

1. AGENCY USE ONLY (*Leave blank*)	2. REPORT DATE	3. REPORT TYPE AND DATES COVERED
	May 2004	Technical Memorandum

4. TITLE AND SUBTITLE

Infrared Heater Used in Qualification Testing of International Space Station Radiators

5. FUNDING NUMBERS

WBS–22–759–30–01

6. AUTHOR(S)

Robert A. Ziemke

7. PERFORMING ORGANIZATION NAME(S) AND ADDRESS(ES)

National Aeronautics and Space Administration
John H. Glenn Research Center at Lewis Field
Cleveland, Ohio 44135–3191

8. PERFORMING ORGANIZATION REPORT NUMBER

E–13928

9. SPONSORING/MONITORING AGENCY NAME(S) AND ADDRESS(ES)

National Aeronautics and Space Administration
Washington, DC 20546–0001

10. SPONSORING/MONITORING AGENCY REPORT NUMBER

NASA TM—2004-212332

11. SUPPLEMENTARY NOTES

Responsible person, Robert A. Ziemke, Plumbrook Station, organization code 7030, 419–621–3216.

12a. DISTRIBUTION/AVAILABILITY STATEMENT

Unclassified - Unlimited
Subject Categories: 14, 18, and 34 Distribution: Nonstandard

Available electronically at http://gltrs.grc.nasa.gov

This publication is available from the NASA Center for AeroSpace Information, 301–621–0390.

12b. DISTRIBUTION CODE

13. ABSTRACT ***(Maximum 200 words)***

Two heat rejection radiator systems for the International Space Station (ISS) have undergone thermal vacuum qualification testing at the NASA Glenn Research Center (GRC), Plum Brook Station, Sandusky, Ohio. The testing was performed in the Space Power Facility (SPF), the largest thermal vacuum chamber in the world. The heat rejection system radiator was tested first; it removes heat from the ISS crew living quarters. The second system tested was the photovoltaic radiator (PVR), which rejects heat from the ISS photovoltaic arrays and the electrical power-conditioning equipment. The testing included thermal cycling, hot- and cold-soaked deployments, thermal gradient deployments, verification of the onboard heater controls, and for the PVR, thermal performance tests with ammonia flow. Both radiator systems are orbital replacement units for ease of replacement on the ISS. One key to the success of these tests was the performance of the infrared heater system. It was used in conjunction with a gaseous-nitrogen-cooled cryoshroud in the SPF vacuum chamber to achieve the required thermal vacuum conditions for the qualification tests. The heater, which was designed specifically for these tests, was highly successful and easily met the test requirements. This report discusses the heating requirements, the heater design features, the design approach, and the mathematical basis of the design.

14. SUBJECT TERMS

Thermal vacuum tests; Heaters; Infrared radiation; International Space Station

15. NUMBER OF PAGES

23

16. PRICE CODE

17. SECURITY CLASSIFICATION OF REPORT	18. SECURITY CLASSIFICATION OF THIS PAGE	19. SECURITY CLASSIFICATION OF ABSTRACT	20. LIMITATION OF ABSTRACT
Unclassified	Unclassified	Unclassified	